ANNALES
UNIVERSITATIS MARIAE CURIE-SKŁODOWSKA
LUBLIN – POLONIA
VOL. LXX SECTIO AAA 2015

ROLE OF THE SHELL AND PAIRING EFFECTS IN NUCLEAR FISSION[1]

Krzysztof Pomorski, Bożena Nerlo-Pomorska

Theoretical Physics Department, Maria Curie-Skłodowska University
pl. M. Curie-Skłodowskiej 1, 20-031 Lublin, Poland

ABSTRACT

The description of spontaneous fission of actinides by the macroscopic-microscopic method consisting of the Lublin Strasbourg Drop model and the two deformed Nilsson wells or the Yukawa folded single-particle potential is presented. The microscopic shell corrections are obtained by the Strutinsky method, while the pairing correlations are taken into account within the BCS theory. It was shown that the pairing strength should grow with increasing deformation of fissioning nucleus in order to obtain right estimates of the pairing field in the fission fragments. The fission barrier heights are estimated using the topographical theorem of Swiatecki.

Keywords: nuclear fission; scission point; barrier heights; shell and pairing effects

1. INTRODUCTION

The nuclear fission was discovered in 1938 by Otto Hahn, Fritz Strassmann [6], and Lisa Meitner [9]. The first theoretical description of this phenomenon was given in 1939 by Niels Bohr and John A. Wheeler [3], but the mechanism of the nuclear, even spontaneous, fission is not fully understood till now. The nuclear fission half-

[1] The paper is devoted to the memory of the late Professor Stanisław Szpikowski

life times $T_{1/2}$ and the origin of asymmetric fission or the kinetic energy distribution of fission fragments need further studies. The shell and pairing corrections in the ground state are crucial for the fission life-times and the barrier heights estimates while the microscopic shell and pairing corrections around the scission point decide about the mass and kinetic energy distribution of the fission fragments. The microscopic corrections were calculated using the single-particle levels of Yukawa folded [4] or Nilsson [16] potentials and added to the macroscopic Lublin Strasbourg Drop [18].

The Strutinsky method [21] was used to obtain the shell correction in the fissioning nucleus and its fragments. It will be shown that the sum of the shell corrections of both fragments is nearly equal to the shell correction evaluated in the mother nucleus even for asymmetric fission.

The pairing correlation were calculated using the BCS theory [1] with the monopole pairing force for the mother nucleus and both fragments. We shall show in the following that the additive property is not fulfilled in asymmetric fission, where the pairing energy of the total system differs from the sum of the pairing energies of the fragments.

It is well known that shape dependent pairing forces switch off the pairing correlations between orbitals in different fragments while it is not the case for the ordinary monopole pairing force. That is why we recommend to use in almost separated system the δ-pairing or the Gogny force [5] instead of the monopole force. We are going also to show that the average pairing energy should grow with deformation in order to reproduce the masses of the fragments after scission. The role of average pairing energy on the fission barrier estimates will be analysed too.

We begin the article with the Lublin Strasbourg Drop (LSD) model [18], which reproduces well the nuclear masses and the fission barrier heights. Then, we present the shell and pairing corrections at large deformations close to the scission point of the fissioning nucleus and show the influence of the average pairing energy on the fission barrier heights of nuclei with $A \approx 100$.

2. NUCLEAR ENERGY OF DEFORMED NUCLEI

2.1. MACROSCOPIC BINDING ENERGY

According to the idea of Meitner and Frisch [9], Bohr and Wheeler [3] have assumed that the liquid drop formula consists of the volume energy, and the deformation dependent surface and Coulomb energy terms:

$$\begin{aligned} E_{LD}(\{\alpha_l\}) &= E_{\rm vol} + E_{\rm surf}(\{\alpha_l\}) + E_{\rm Coul}(\{\alpha_l\}) \\ &= a_{\rm vol}A + a_{\rm surf}A^{2/3}B_{\rm surf}(\{\alpha_l\}) + \tfrac{e^2\chi^2}{r_0A^{1/3}}B_{\rm Coul}(\{\alpha_l\}), \end{aligned} \tag{1}$$

where $\{\alpha_l\}$ is a set of expansion coefficients of nuclear radius in Legendre polynomials P_l series

$$R(\theta) = R_0(\{\alpha_l\}) \left(1 + \sum_{l=0}^{\infty} \alpha_l P_l(\theta)\right). \tag{2}$$

Here $R_0(\{\alpha_l\})$ is the radius of a deformed nucleus which has the same volume as the spherical one.

Analysing the liquid drop potential energy surface, Bohr and Wheeler have shown that the saddle point of the liquid drop energy function in the $\{\alpha_l\}$ deformation parameters space appears at large deformation α_2 and the fission barrier occurs when the fissility parameter

$$x = \frac{E_{\text{Coul}}(0)}{2E_{\text{surf}}(0)} \approx \frac{Z^2}{50A}\text{MeV} \tag{3}$$

is smaller than 1, what is clearly seen when one expands the relative to sphere surface and Coulomb energies in the Taylor series with respect to the deformation parameters:

$$B_{\text{surf}} = 1 + \frac{2}{5}\alpha_2^2 + \frac{5}{7}\alpha_3^2 + \ldots \quad ; \qquad B_{\text{Coul}} = 1 - \frac{1}{5}\alpha_2^2 - \frac{10}{49}\alpha_3^2 - \ldots \tag{4}$$

The shell effects were included to the deformed macroscopic potential energy surface in 1966 by Myers and Swiatecki who have proposed a phenomenological formula for the shell correction energy [13] and reproduced with a good accuracy the known at that time nuclear masses. After appearance of this first macroscopic-microscopic model [12] several more complex macroscopic formulae containing more adjustable parameters were developed: the droplet model [13], the Yukawa-plus-exponential anzatz [7], the finite-range droplet model [10] or the Thomas-Fermi theory [14]. Surprisingly, it was shown in Ref. [18] that a simple liquid drop formula containing in addition to Eq. (1) the surface curvature term is able to reproduce both the experimental binding energies and the fission barrier height with even better accuracy that the above more complicated models with the same microscopic energy corrections. This Lublin Strasbourg Drop (LSD) mass formula [18] reads:

$$\begin{aligned} M_{\text{mac}}(Z,N;\text{def}) &= ZM_{\text{H}} + NM_{\text{n}} - b_{\text{elec}}Z^{2.39} + b_{\text{vol}}\left(1-\kappa_{\text{vol}}I^2\right)A \\ &+ b_{\text{surf}}\left(1-\kappa_{\text{surf}}I^2\right)A^{2/3}B_{\text{surf}}(\text{def}) + b_{\text{cur}}\left(1-\kappa_{\text{cur}}I^2\right)A^{1/3}B_{\text{cur}}(\text{def}) \\ &- \tfrac{3}{5}\tfrac{e^2Z^2}{r_0^{\text{lab}}A^{1/3}}B_{\text{Coul}}(\text{def}) - C_4\tfrac{Z^2}{A} + E_{\text{cong}}(Z,N;\text{def}). \end{aligned} \tag{5}$$

where the congruence energy E_{cong} is defined in Ref. [15]. The mass of a nucleus composed of Z protons and N neutrons is

$$M(Z,N;\text{def}) = M_{\text{mac}}(Z,N;\text{def}) + E_{\text{micr}}(Z,N;\text{def}). \tag{6}$$

The microscopic part of the binding energy E_{micr} consists of the shell δE_{shell} and pairing δE_{pair} energy corrections

$$E_{\rm micr}(Z.N;{\rm def}) = \delta E_{\rm shell}(Z,A;{\rm def}) + \delta E_{\rm pair}(Z.A;{\rm def})\,. \tag{7}$$

One can obtain the microscopic energy corrections using e.g. the Nilsson [16, 17], the Saxon-Woods [22] or the Yukawa-folded [4] single-particle potentials and the Strutinsky method to evaluate the shell energy corrections [21, 17], while the BCS theory is used to get the pairing correlations energy [1, 17].

All results presented below were obtained using the LSD macroscopic energy model with the curvature term [18] as shown in Eq. (5) and the Nilsson [16, 17] or the Yukawa-folded [7, 10] single-particle potentials .

2.2. SHELL CORRECTION

The Strutinsky shell energy is given by the following difference:

$$\delta E_{\rm shell} = \sum_{occ} 2e_\nu - \tilde{E}_{\rm Str}\ , \tag{8}$$

where the sum goes over all occupied single-particle (s.p.) energies e_ν and the second term is the smoothed s.p. energy sum which can be calculated by the Strutinsky prescription [21, 17]. The total shell-energy consists of the proton and neutron contributions. The average sum of the single-particle energies is given by the integral

$$\tilde{E}_{\rm Str} = \int_{\infty}^{\tilde{\lambda}} 2\,e\,\tilde{g}(e)\,de\ , \tag{9}$$

where $\tilde{g}(e)$ is the smooth level density obtained by folding the real spectrum of the single-particle energies

$$g(e) = \sum_\nu \delta(e-e_\nu) \quad \longrightarrow \quad \tilde{g}(e) = \frac{1}{\gamma_S}\sum_\nu j_n\left(\frac{e-e_\nu}{\gamma_S}\right). \tag{10}$$

with Gauss function multiplied by the sixth order [17]

$$j_6(x) = \frac{1}{\sqrt{\pi}}e^{-x^2}\left(\frac{35}{16} - \frac{35}{8}x^2 + \frac{7}{1}x^4 - x^6\right). \tag{11}$$

or higher order correction polynomial. The smearing parameter γ_s should be of the order of the distance between the major shells to wash out the shell effects in $\tilde{E}$ and ensure the plateau condition (independence on γ_S) of the shell energy. One obtains the average Fermi energy $\tilde{\lambda}$ in Eq. (9) from the particle number equation in the system with the smoothed shell structure

$$\mathcal{N} = \int_{-\infty}^{\tilde{\lambda}} 2\,\tilde{g}(e)\,de\,. \tag{12}$$

An alternative to the Strutinsky approach is the averaging of the single-particle energy sum over the number of particles (see e.g. [19]). This method leads to similar

magnitudes of the shell energy corrections for deformed nuclei while for the spherical ones absolute values of the negative energy corrections are larger.

2.3. ADDITIVE PROPERTY OF THE SHELL CORRECTIONS

Let us assume that we are dealing with the almost separated fission fragments. The single-particle potential well of such system is schematically presented in Fig. 1. The bound single-particle levels, which one obtains after diagonalization of the Hamiltonian with such a potential, are already localised in the two wells corresponding to each fission fragment. Only the weakly bound and unboud states have wave functions which are distributed over the whole system.

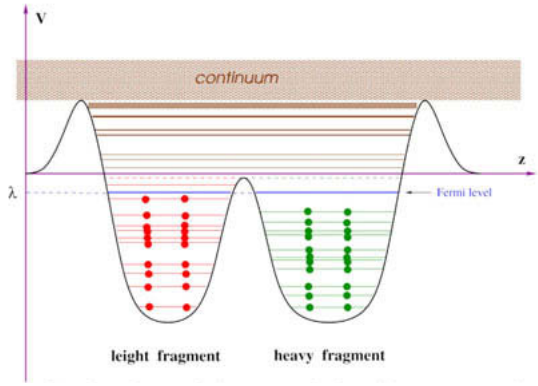

Figure 1: Schematic plot of a single-particle potential well corresponding to the two almost separated fission fragments.

The common energy spectrum of the bound states can be separated into the levels belonging to the heavy or to the light fragment: $\{e\} \equiv \{e^l, e^h\}$. Both fragments should have the same average Fermi energy (12) as the mother nucleus because the system is not yet fully divided: $\tilde{\lambda}^l = \tilde{\lambda}^h = \tilde{\lambda}$. For such a configuration the following relations can be written:

$$\widetilde{E}_{\rm Str} = \widetilde{E}^l_{\rm Str} + \widetilde{E}^h_{\rm Str} \quad \text{and} \quad \mathcal{N} = \mathcal{N}^l + \mathcal{N}^h \ . \tag{13}$$

So

$$E_{shell} = \sum_{occ} 2e_\nu - \widetilde{E}_{\rm Str} = \sum_{occ} 2e^l_\nu + \sum_{occ} 2e^h_\nu - \widetilde{E}^l_{\rm Str} - \widetilde{E}^h_{\rm Str} \tag{14}$$

and

$$E_{shell} = E^l_{shell} + E^h_{shell} \tag{15}$$

2.4. PAIRING CORRECTION

The pairing correction is defined as the difference between the BCS and the average pairing energy

$$\delta E_{\rm pair} = E_{\rm pair} - \langle E_{\rm pair} \rangle \tag{16}$$

The average pairing correlation energy was supposed to be already contained in the macroscopic part of the binding energy [12], which is not necessarily true. We shall point this later in Sec. 3. The pairing energy $E_{\rm pair}$ is equal to the difference of the BCS [1] energy and the sum of the energies of the occupied single-particle levels: [17]

$$E_{\rm pair} = E_{\rm BCS} - \sum_{occ} 2e_\nu \ , \tag{17}$$

where

$$E_{\rm BCS} = \sum_\nu 2v_\nu^2 e_\nu - G\sum_\nu u_\nu v_\nu - G\sum_\nu v_\nu^4 \tag{18}$$

G is the pairing strength, v_ν and u_ν are the occupation and unoccupation BCS factors.

2.5. ADDITIVE PROPERTY OF THE PAIRING CORRECTIONS

In the case of the pairing energy, the average pairing gaps could be different in both fragments. Let us consider a nucleus composed of two almost separated fragments in which the pairing correlations are described by the monopole pairing Hamiltonian:

$$\widehat{H} = \widehat{H}_0 + \widehat{H}_{pair} = \sum_\nu e_\nu \left(a_\nu^+ a_\nu + a_{\bar\nu}^+ a_{\bar\nu}\right) - G\sum_{\nu,\mu} a_\nu^+ a_{\bar\nu}^+ a_{\bar\mu} a_\mu \ , \tag{19}$$

where a_ν^+ and a_ν the particle creation and annihilation operators and $\bar\nu$ denotes a time reversal single-particle state. One can define the operators of annihilation of a pair of particles in each fragment (l-light or h-heavy):

$$\hat{P}_l = \sum_\nu a_{\bar\nu}^l a_\nu^l \quad \text{and} \quad \hat{P}_h = \sum_\nu a_{\bar\nu}^h a_\nu^h \ . \tag{20}$$

and corresponding creation operators $\hat{P}_l^+ = (\hat{P}_l)^+$ and $\hat{P}_h^+ = (\hat{P}_h)^+$. The single-particle and pairing Hamiltonian in the new operators takes the following form:

$$\widehat{H} = \widehat{H}_0^l + \widehat{H}_0^h - G_l\hat{P}_l^+\hat{P}_l - G_h\hat{P}_h^+\hat{P}_h - G_{lh}\left(\hat{P}_l^+\hat{P}_h + P_h^+\hat{P}_l\right). \tag{21}$$

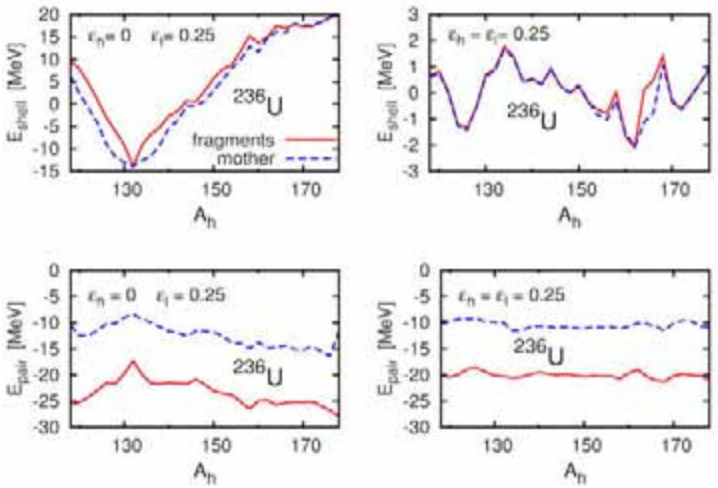

Figure 2: Sum of the shell energies of fragments (solid line) and the shell energy of the mother nucleus ^{236}U (dotted line) as functions of the heavy fragment mass (upper row). Similar data but for the pairing energy are plotted in the bottom row. Left column corresponds to spherical heavy fragment and prolate light one while the r.h.s column shows the results when both fragments are prolate.

The monopole pairing strength G is in the first approximation proportional to $1/A$, so in the case of the separated fragments the approximation $G_l = G_h = G_{lh} = G$ is not valid any more. One should rather assume: $G_l \geq G_h > G$ and $G_{lh} \approx 0$, where the equality sign is valid for the symmetric fission only.

The BCS equations for almost separated fragments will take the following form:

$$\frac{2}{G} = \sum_{\nu} \frac{1}{E_\nu} \neq \sum_{\nu} \frac{1}{E^l_\nu} + \sum_{\nu} \frac{1}{E^h_\nu} = \frac{2}{G_l} + \frac{2}{G_h} \tag{22}$$

and

$$N = \sum_{\nu} 2v^2_\nu = \sum_{\nu} 2(v^l_\nu)^2 + \sum_{\nu} 2(v^h_\nu)^2 = N_l + N_h \ , \tag{23}$$

where

$$E^l_\nu = \sqrt{(e^l_\nu - \lambda_l)^2 + \Delta^2_l} \ , \qquad (v^l_\nu)^2 = \frac{1}{2}\left(1 - \frac{e^l_i - \lambda_l}{E^l_i}\right) \ , \quad \text{etc.} \tag{24}$$

with $\Delta \neq \Delta_l \neq \Delta_h$ and $\lambda \approx \lambda_l \approx \lambda_h$.

2.6. ADDITIVE PROPERTY OF MICROSCOPIC CORRECTIONS

In Fig. 2 the two deformed Nilsson [17] wells are used to describe the configuration of the fission fragments. The shell (upper row) and the pairing (bottom row) energy of the mother system (dashed lines) are compared with the sum of the shell energies (solid lines) of the both fragments of ^{236}U for different mass ratios and

two different shapes of the fragments. It is seen in Fig. 2 that the shell energy of the mother nucleus is nearly equal to the sum of the fragments shell energies as it should be according to Eq. (15). The pairing energy is almost doubled in the fragments as can be visible in the two bottom plots in Fig. 3. This is in agreement with results obtained in Ref. [20] for the systems without shell structure. In the plot we haven't subtracted the average pairing energy nor the pairing diagonal term. The pairing strengths for the mother nucleus and fission fragments was adjusted to the average experimental proton and neutron gaps: $\bar{\Delta}^{(p)}_{\rm exp} = 4.8Z^{-1/3}$ MeV and $\bar{\Delta}^{(n)}_{\rm exp} = 4.8N^{-1/3}$ MeV taken from Ref. [11].

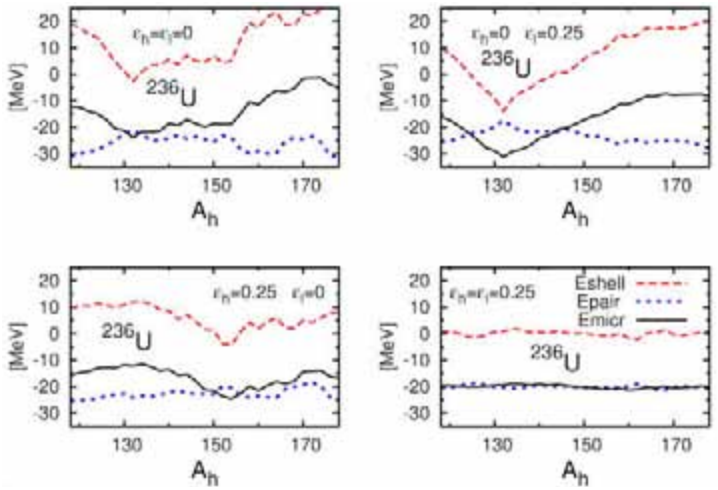

Figure 3: Shell energy (dashed line), the sum of the pairing energies of the fragments (dotted line) and the total microscopic energy (solid line) as functions of the heavy fragment mass A_h. The results are drawn for four elongations ε_h, ε_l of heavy and light fragment (written in the plots).

The total value of the microscopic energy as well as its both components $E_{\rm shell}$ and $E_{\rm pair}$ are plotted in Fig. 3 as functions of the heavy fragment mass. Each of four plots corresponds to a different deformations of the fission fragments. We have switched off the pairing interaction between orbitals belonging to different fragments. This can be done automatically when one uses e.g. the δ-pairing force [8] instead of the monopole pairing interaction

$$V^q(\vec{r}_1,\vec{\sigma}_1;\vec{r}_2,\vec{\sigma}_2) = V_0^q \frac{1-\vec{\sigma}_1\cdot\vec{\sigma}_2}{4}\delta(\vec{r}_1-\vec{r}_2)\,, \quad \text{with} \quad q=n,p\,, \tag{25}$$

where V_0^q is the δ pairing strength, $\vec{\sigma}_1$ and $\vec{\sigma}_2$ denote Pauli matrices of protons and neutrons. Matrix elements of the δ-pairing force are:

$$V_{i\bar{i}j\bar{j}} = V_0^q \int d^3r \rho_i^q(\vec{r})\rho_j^q(\vec{r})\,, \tag{26}$$

where $\rho_i^q(\vec{r}) = |\varphi_i^q(\vec{r})|^2$, where φ_i^q is the single-particle wave function. It means that the matrix elements (26) vanish when the orbits φ_i^q and φ_j^q belong to the different fragments. One obtains similar effect in case of the Gogny interaction [5] frequently used in the self-consistent Hartee-Fock-Bogolubov calculations.

3. CONGRUENCE AND THE AVERAGE PAIRING ENERGIES

In the macroscopic-microscopic model one usually assumes that the average pairing energy is contained in the macroscopic part of the binding energy. To check the validity of this assumption one has evaluated in Ref. [20] the average monopole pairing energy of nuclei from different mass regions at small deformations corresponding to the ground state and at the scission configurations. The proportional to v_ν^4 term in Eq. 18 was taken into account when evaluating the pairing energy.

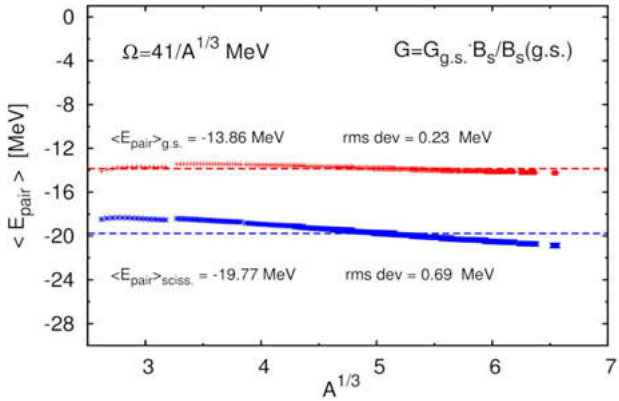

Figure 4: Average pairing energy of nuclei at the ground state and at the scission point in function of $A^{1/3}$. Here, the pairing strength is proportional to the surface of deformed nucleus and Ω denotes the frequency of the spherical harmonic oscillator in the Nilsson type potential (After [20]).

The results are presented in Fig. 4. One can see that the average pairing energy in the ground state is almost A-independent and approximately equal to -14 MeV. This result means that the average-pairing should be doubled when two fission fragments are born from the mother nucleus. There is no mechanism in the macroscopic-microscopic model which can give this effect. The only remedy is to assume that the average-pairing energy should not be included into the macroscopic energy. In addition one has to take the deformation dependent monopole-pairing strength or more complex pairing force as discussed in the previous section. The taking into account only the fluctuative part of the pairing energy $\delta E_{\rm pair}$ leads only to a systematic error in the deformation dependence of the macroscopic-microscopic energy. One has to add to the macroscopic energy $E_{\rm macr}$ the whole pairing energy

(17) not only its fluctuating part in order to get proper estimates of the binding energy at the saddle-point as well as at the scission configuration.

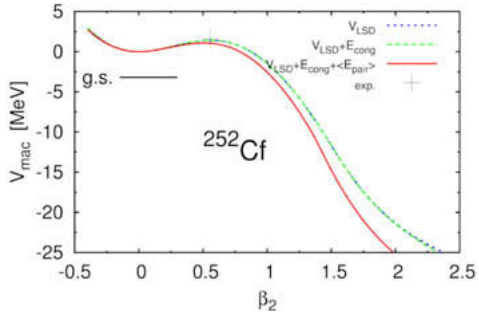

Figure 5: Macroscopic fission barrier $V_{\rm mac}({\rm def}) = M_{\rm mac}({\rm def}) - M_{\rm mac}({\rm sph})$ of ^{252}Cf isotope as function of the quadrupole deformation of nuclei. The barrier is evaluated using the LSD energy (dotted line) minimised with respect to higher multipolarity deformations $\beta_\lambda\,(\lambda = 4, 6, ...16)$ and with taking into account the deformation dependence of the congruence energy (dashed lines) and the average-pairing terms (solid line). The cross corresponds to the experimental fission barrier height reduced by the microscopic effects at the ground-state according to the topographical theorem [14].

It was shown in Ref. [20] that the proportional to the surface monopole pairing strength ($G \sim S$) can roughly give the doubling effect of the pairing energy at scission. It is seen in Fig. 4 that the magnitude of $< E_{\rm pair} >$ evaluated with $G \sim S$ at the scission configuration is much larger (almost twice for the heaviest nuclei) than in the ground-state.

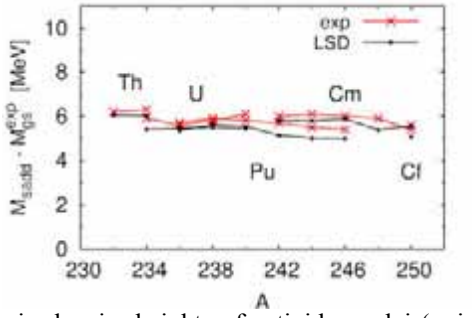

Figure 6: LSD fission barrier barrier heights of actinide nuclei (points) compared with the data (crosses). The topographical theorem [14] was used to obtain these estimates.

Similar effect but for the congruence (Wigner) energy was already noticed in Ref. [15], where one has assumed that the congruence energy at the scission point is twice as large as in the ground state. The effect of deformation dependent congruence and average pairing energy on the fission barrier heights was discussed in Ref. [20] and is shown in Fig. 5 for Br to Cf isotopes. It is seen in Fig. 5 that the deformation dependent average-pairing and congruence energies do not change

much the barrier height of heavy nuclei but significantly approach the estimates of the fission barrier heights to their measured values as shown in Ref. [20].

The barrier heights were estimated using the topographical theorem of Swiatecki in which one assumes that the binding energy of nucleus at the saddle is mostly determined by the macroscopic part of the binding energy. The quality of this approximation can be seen in Fig. 6, where the experimental fission barrier heights of 18 actinide nuclei are compared to their estimates in which the LSD macroscopic mass formula was used to evaluate the mass of nuclei at the saddle point which was determined within the MFH shape parametrisation [2]. All estimates except one (^{252}Cf) are slightly below the data (r.m.s. 310 keV) what leaves a place for the small unwashed shell effects at the saddle.

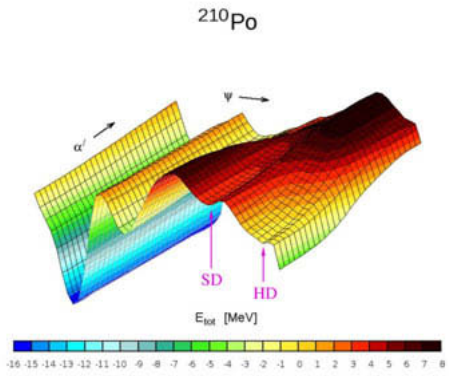

Figure 7: Potential energy surface of ^{210}Po in elongation ψ and asymmetry α' plane.

4. POTENTIAL ENERGY SURFACE

The potential deformation energy of a nucleus is equal:

$$E_{\rm tot}({\rm def}) = M_{\rm mac}({\rm def}) + \delta E_{shell}({\rm def}) + \delta E_{pair}({\rm def}) - M_{\rm mac}({\rm sph}) \qquad (27)$$

An example of results of the potential energy surface of ^{210}Po isotope is presented in Fig. 7. The calculation was done with the Yukawa-folded (YF) single-particle potential and LSD macroscopic energy using the Modified Funny-Hills shape parametrization of the deformed nucleus shapes [2]. The parameter ψ corresponds to the elongation of fissioning nucleus while α' describes the mass asymmetry mode. One can see that the second barrier is significantly reduced by the reflection asymmetry, while the super-deformed (SD) and hyper-deformed (HD) minima are on the path which corresponds to the symmetric in mass fission. One has to stress here that the proper choice of the shape parametrization was very important to obtain the shell effects at such very elongated shapes. The right hand side end of the potential energy surface corresponds to the liquid drop scission line.

5. CONCLUSIONS

The following conclusions can be drawn from our investigations:

- The sum of shell energies of the fission fragments is close to the shell energy of the mother system around the scission configuration.
- The sum of pairing energies of the fission fragments could be different from the pairing energy evaluated for the common system close to the scission configuration corresponding to the symmetric fission.
- The deformation dependent congruence energy and the pairing strength proportional to the nuclear surface improve the estimates of the barrier heights of the light nuclei.
- The average pairing energy of fissioning nucleus should grow with deformation to the double value at the scission point.
- Lublin Strasbourg Drop describes well masses of all isotopes both in the ground state and saddle points.

ACKNOWLEDGEMENTS

The work was partly supported by the Polish National Science Centre, under the grant No. 2013/11/B/ST2/04087.

REFERENCES

1. Bardeen J., Cooper L.N., Schrieffer J.R., 1957. Theory of Superconductivity, Physical Review 108, 1175–1204.
2. Bartel J., Nerlo-Pomorska B., Pomorski K., Schmitt C., 2014. The potential energy surface of 240Pu around scission, Physica Scripta 89, 054003, 1–5.
3. Bohr N., Wheeler J.A., 1939. The Mechanism of Nuclear Fission, Physical Review 56, 426–450.
4. Bolsterli M., Fiset E.O., Nix J.R., Norton L., 1972. New Calculation of Fission Barrier for Heavy and Superheavy Nuclei, Physical Review C 5, 1050–1078.
5. Gogny D., 1975. in "Nuclear Self Consistent Fields", Ripka G. and Porneuf M. (Eds.), North Holland, Amsterdam, p. 333.
6. Hahn O., Straßmann F., 1939. Über den Nachweis und Verhalten der bei der Bestrahlung des Urans mittels Neutronen entstehenden Erdalkalimetale, Naturwissenschaften 27, 11–15.
7. Krappe H.J., Nix J.R., Sierk A.J., 1979. Unified nuclear potential for heavy-ion elastic scattering, fusion, fission, and ground-state masses and deformations, Physical Review C 20, 992–1013.
8. Krieger S.J., Bonche P., Flocard H., Quentin P., and Weiss M., 1990. An improved pairing interaction for mean field calculations using Skyrme potentials, Nuclear Physics A517, 275–284.
9. Meitner L., Frisch O.R., 1939. Disintegration of Uranium by Neutrons: a New Type of Nuclear Reaction, Nature 143, 239–240.

10. Möller P., Myers W.D., Swiatecki W.J., Treiner J., 1988. Nuclear mass formula within a finite-range droplet model and folded-Yukawa single-particle potential, Atomic Data and Nuclear Data Tables 39, 225.
11. Möller P., Nix J.R., 1992. Nuclear pairing model, Nuclear Physics A536, 20–60.
12. Myers W.D., Swiatecki W.J., 1966, Nuclear Masses and Deformations, Nuclear Physics 81, 1–60.
13. Myers W.D., Swiatecki W.J., 1969. Average Nuclear Properties, Annals of Physics 55, 395–505; *ibid*. 1974. Nuclear Droplet Model for Arbitrary Shapes, Annals of Physics 84, 186–210.
14. Myers W.D., Swiatecki W.J., 1996. Nuclear properties according to the Thomas-Fermi model, Nuclear Physics A601, 141–167.
15. Myers W.D., Swiatecki W.J., 1997. The congruence energy: a contribution to nuclear masses, deformation energies and fission barriers, Nuclear Physics A612, 249–261.
16. Nilsson S.G., 1955. Binding states of individual nucleons in strongly deformed nuclei, Det Kongelige Danske Videnskabernes Selskab Matematisk-fysiske Meddelelser 29, no. 16, 1–70.
17. Nilsson S.G., Tsang C.F., Sobiczewski A., Szymanski Z., Wycech S., Gustafson C., Lamm I.L., Möller P. and Nilsson B., 1969. On the nuclear structure and stability of heavy and superheavy elements, Nuclear Physics A131, 1–66.
18. Pomorski K., Dudek J., 2003. Nuclear liquid-drop model and surface-curvature effects, Physical Review C 67, 044316, 1–13.
19. Pomorski K., 2004. Particle number conserving shell-correction method, Physical Review C 70, 044306, 1–10.
20. Pomorski K., Ivanyuk F., 2009. Pairing correlations and fission barrier heights, Int. Journal Modern Physics E18, 900–906.
21. Strutinsky V.M., 1967. Shell effects in nuclear masses and deformation energies, Nuclear Physics, A95, 420–442 ; 1968. Shells in deformed nuclei, Nuclear Physics A122, 1–33.
22. Woods R.D., Saxon D.S., 1954. Diffuse Surface Optical Model for Nucleon-Nuclei Scattering Physical Review 95, 577–578.